

AperTO - Archivio Istituzionale Open Access dell'Università di Torino

### WO3 nanorolls self-assembled as thin films by hydrothermal synthesis

**This is the author's manuscript**

*Original Citation:*

*Availability:*

This version is available <http://hdl.handle.net/2318/1508987> since 2015-12-02T16:41:32Z

*Published version:*

DOI:10.1039/c4nr07290a

*Terms of use:*

Open Access

Anyone can freely access the full text of works made available as "Open Access". Works made available under a Creative Commons license can be used according to the terms and conditions of said license. Use of all other works requires consent of the right holder (author or publisher) if not exempted from copyright protection by the applicable law.

(Article begins on next page)



# UNIVERSITÀ DEGLI STUDI DI TORINO

***This is an author version of the contribution published on:***

*Questa è la versione dell'autore dell'opera:*

*Nanoscale*, 2015, 7, 7174-7177, 2015 <http://dx.doi.org/10.1039/c4nr07290a>

***The definitive version is available at:***

*La versione definitiva è disponibile alla URL:*

<http://pubs.rsc.org/en/Content/ArticleLanding/2015/NR/C4NR07290A#!divAbstract>

# WO<sub>3</sub> Nanorolls Self-Assembled as Thin Films by Hydrothermal Synthesis

S. Vankova<sup>a</sup>, S. Zanarini<sup>a\*</sup>, J. Amici<sup>a</sup>, F. Cámara<sup>b,c</sup>, R. Arletti<sup>b,c</sup>, S. Bodoardo<sup>a\*</sup>, N. Penazzi<sup>a</sup>

Received (in XXX, XXX) Xth XXXXXXXXXX 20XX, Accepted Xth XXXXXXXXXX 20XX

DOI: 10.1039/b000000x

We report a Novel type of WO<sub>3</sub> nanostructure, i.e. nanorolls obtained as self-assembled thin film on a transparent conductive substrate. The mild conditions of preparation, avoiding the use of HCl, result in a eco-friendly hydrothermal method with reduced crystallization time. FESEM and HR-TEM show that WO<sub>3</sub> nanocrystals are made of rolled nanoflakes with a telescope-like appearance in their tip. For their nano-porosity, electrochemical accessibility, good adhesion to substrate and the envisaged presence of nanocavities between WO<sub>3</sub> layers, these material hold tremendous promise for nano-electronics, electrochromic devices, water photo-splitting cells, Li-ion batteries and nano-templated filters for UV radiation.

Nanostructured thin films of WO<sub>3</sub> hold currently a pivotal role in different fields as energy efficient buildings<sup>1,2</sup>, flexible power saving displays<sup>3</sup>, light driven water oxidation<sup>4,5</sup>, Li-ion batteries<sup>6</sup> and nano-electronics<sup>7</sup>. Tungsten oxide has been one of the first and more widely studied electrochromic inorganic materials<sup>8,9</sup>. In the last years several types of WO<sub>3</sub> nanocrystals have been developed<sup>10,11,12,13,14,15,16</sup>. A simple and customizable solvothermal technique to prepare WO<sub>3</sub> nanowires and nanoflakes arrays directly on Fluorine-doped tin oxide was recently reported by Su<sup>17</sup>. In the last months<sup>18</sup> the possibility to avoid the seed layer pre-deposition has been also demonstrated by the use of WO<sub>3</sub>•0.33H<sub>2</sub>O; another method to introduce easily Metal nanoparticles in Urchin-like WO<sub>3</sub> nanostructures was recently demonstrated<sup>19</sup>. In the direction of the flexibility on the nano layer, very recently wearable electrochromic devices were obtained by depositing WO<sub>3</sub> on a layer of silvers nanowires<sup>20</sup>. Starting from the recent advances in the hydrothermal (HT) preparation of WO<sub>3</sub> nanoflakes, we report a novel type of electrochromic nanocrystal, namely WO<sub>3</sub> nanorolls (NR), grown in two steps as thin films on FTO/glass substrate. WO<sub>3</sub> Nanorolls are fibrous multi-layer structures with nano-cavities between single foils and envisaged multiple exploitation directions in nano-electronics, water photo-splitting cells, Li-ion batteries and nano-templated filters for UV radiation. The previously unreported nanostructure has been obtained by modifying the Su method<sup>17</sup>. It is worthy to note that in general in HT preparation small changes in pH, reactants concentration, reaction time and temperature can affect substantially the nanocrystal growth. Here starting from Su method, the WO<sub>3</sub> NR were obtained by

avoiding the use of HCl (pH=1 instead of -0.73) and by limiting the reaction time to 3 h instead of 6 resulting in a eco-friendly and quick HT process. The nanoscale morphology of WO<sub>3</sub> NR is reproducible and can be tuned by changing the polyvinyl alcohol (PVA) chain length during seed layer preparation as discussed in detail below. In the first step, a sol-gel method was adopted to produce a WO<sub>3</sub> seed layer on the FTO/Glass surface, which is fundamental to address the geometry of crystallization and the pattern of substrate coverage. 1.25 g of H<sub>2</sub>WO<sub>4</sub>, 0.5 g of PVA (from Sigma-Aldrich), and 10 mL of 50% H<sub>2</sub>O<sub>2</sub> were mixed and stirred for 30 minutes at room temperature, producing a yellow colloidal solution. This solution was spin-coated at 100 rps into FTO/glass substrate; the sample was then heated at 500 °C for 2h to remove the organic component and to decompose (PVA)<sub>2</sub>[WO<sub>2</sub>(O<sub>2</sub>)<sub>2</sub>] precursor to WO<sub>3</sub>. The second step consisted in the in-situ Hydrothermal growing of WO<sub>3</sub> nanorolls on the WO<sub>3</sub> seed layer in mild conditions. 15 ml of Tungstic acid (H<sub>2</sub>WO<sub>4</sub>) 0.05 M, 12.5 ml of distilled H<sub>2</sub>O, and 0.150 g of oxalic acid were added to 60 ml of acetonitrile. The raw materials were mixed and stirred at RT for 10 minutes. The resulting solution (pH = 1) was poured into the vessel of a Teflon lined autoclave. The WO<sub>3</sub>/FTO/glass substrates were then placed in the reaction vessel with the WO<sub>3</sub> seed layer facing upward at 180 °C for 3 h. The samples were then cleaned with ethanol and distilled water, and dried at room temperature for 1 h (See Figure S1 for the typical layer by layer FESEM cross section). FESEM pictures (Figure 1) show that the sample has fibers few hundreds of nanometers long in a moderate parallel organization with the fibers pointing approximately up in a narrow size distribution. At large magnification is evident that these fibrous structures appear as discontinuously rolled sheets that can be called nanorolls. Powder XRD revealed that WO<sub>3</sub> NR are composed of hexagonal WO<sub>3</sub>, with some reflections coming from the FTO substrate (Figure S2). Refinement of the hexagonal WO<sub>3</sub> cell yielded *a* 0.734(2) nm, *c* 0.763(2) nm and *V* = 0.356 nm<sup>3</sup>. A cell with halved *c* lattice can be also fitted by HR-TEM show that a faint disordered *c* periodicity at 0.763 nm. observations. Figure 2a shows HR-TEM images of a nanoroll fragment. Most of nanorolls are formed by multilayer aggregates. Fourier transform of images show that nanorolls are elongated along [001] and have [100] parallel to the nanoroll surfaces. Streaking along [100] is related to the curvature of the foils. When the nanoroll fragments are thinner a more ordered pattern is observed (see FFT inset in Figure 2b obtained from the lower left image, where faint 001

periodicities are observed).

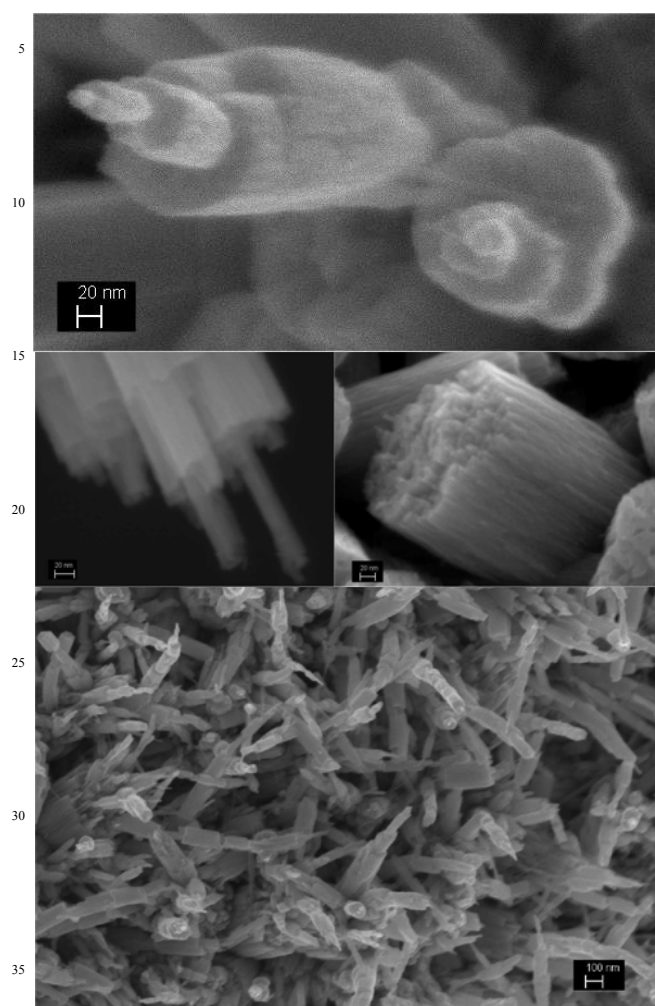


**Figure 1.** FESEM images of the run product showing the rolled  $\text{WO}_3$  sheets with envisaged nanocavities between layers.

After few minutes of observation some thin layers may eventually detach (black arrow in upper right image in Figure 2b). A previous work suggested that  $\text{Li}^+$  is incorporated through migration along [001]-hexagonal channels<sup>21,22</sup>. More recently it has been hypothesized that  $\text{Li}^+$  is located in square windows perpendicular to hexagonal windows<sup>23</sup>. The observed orientation of the foils is consistent with a large exposure of square windows to the external areas of the nanorolls, increasing the possibility of  $\text{Li}^+$  exchange.

The effect of the preparative conditions on the single  $\text{WO}_3$  nanoroll morphology has been investigated by FESEM imaging; three different PVA chain lengths have been tested in seed layer preparation i. e. 31000-50000, 85000-124000 and 146000-186000 UMA. To try measuring the diameter and length of single  $\text{WO}_3$  NR the samples have been observed in two different ways i.e. as obtained on FTO glass and by scratching away the thin layer on Lacey Carbon/200 nm Cu mesh (SPI Supplies). In particular the estimation of the length of a single nanoroll fiber is quite difficult. If we consider the prepared sample in fact the

single NR are quite tangled with a prevalent upright orientation preventing the possibility to estimate their length (Figure 1). Additionally if one try to isolate single fibers by removing mechanically the thin

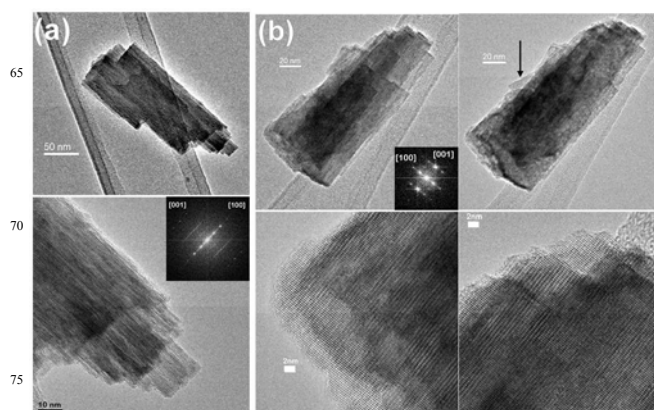


**Figure 2.** HR-TEM images of nanoroll fragments: (a) detail showing superimposed foils with disordering along [100] due to curvature; (b) another nanoroll fragment showing thinner areas in which is possible observe ordered areas – after observation, from the nanoroll fragment (upper left) a foil is detached (marked with a black arrow in upper right).

layer from the underlying FTO substrate, nanorolls fibers are fragmented (see Figure S3 ). Anyway an approximate estimation of the diameter and length of NR as function of the PVA chain length during HT preparation has been obtained by at least 20 different single quite well visible NR (see Figure S4) and reported in Table S1. It is interesting to note that in general nanorolls fibers show two different regions i.e. the portion close to substrate that we call log and the lower diameter ending segment i. e. the tip. Due to this spontaneous segmentation the diameter and length of the log and the tip are indicated separately in table S1. The effect of the PVA chain length on the morphology of the single  $\text{WO}_3$  NR is well visible in Figure 3 and S3. By increasing PVA molecular weight the seed layer is progressively more rough as evidenced by the lower stability of nanostructured layer that is more easily detached during electrochemical testing. In fact the NR log tend to reduce its diameter (about 100 nm) affecting the adhesion to substrate and the tip is not clearly distinguishable while NR fibers tend to be longer (900 to 1200 nm ca.). When the lower molecular weight PVA is employed (Figure S3 left) the NR log diameter is larger (ca. 200-250 nm) the overall fiber length is reduced (500-600 nm) and the log/tip length ratio is high; in this case due to the enhanced surface of contact with the substrate and to the solidity of the massive logs the thin film stability is much higher. For intermediate PVA chain lengths interestingly the thin tip appears longer (diameter 20-40 nm) with respect to log (diameter of 100-150 nm, Figure 3). The  $\text{WO}_3$  NR sheet resistance  $R_s$  has been measured by a four collinear, equally spaced contacts<sup>24</sup>. The total measured resistance  $R_T = 8.06 \Omega/\text{sq}$ , is due to the parallel between the  $\text{WO}_3$  NR film and the conducting substrate resistance. Taking into account the measured substrate resistance (glass with FTO)  $R_{\text{FTO}} = 13.73 \Omega/\text{sq}$ , the  $\text{WO}_3$  NR sheet resistance is  $R_{\text{NR}} = 19.5 \Omega/\text{sq}$ , and is the same for all the three PVA chain lengths showing interestingly a moderate lateral conductivity probably supported

by the tangled structure of NR. The electrolyte ionic conductivity ( $R_{EL}$ ) and the  $WO_3$  NR/FTO thin film polarization resistance ( $R_{POL}$ ) were determined by electrochemical impedance spectroscopy analysis at ambient temperature in PC 1M LiTFSi solution (See Figure S5 for the typical Nyquist Plot). By analysing samples with different PVA chain length, values of  $R_{EL}$ = 25-35  $\Omega$  and  $R_{POL}$ =120-200  $\Omega$  were estimated.

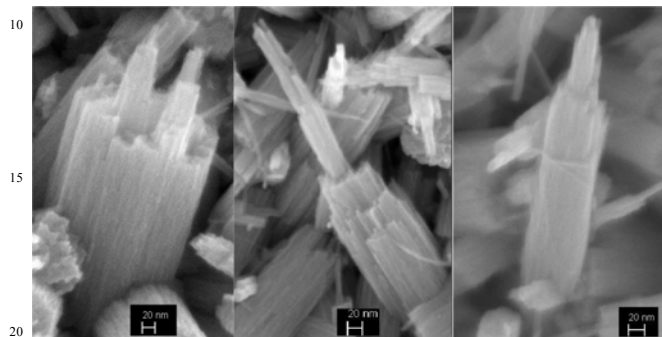


**Figure 3.** FESEM pictures showing the effect of PVA chain length on the sub-structure morphology of a nanoroll fiber. PVA molecular weight is increasing from left to right.

The typical Cyclic voltammogram of  $WO_3$  Nanorolls on FTO substrate in 1 M LiTFSi/PC electrolyte is shown in Figure 4. The shape and position of the oxidation and reduction processes are in good agreement with the literature<sup>25</sup> with a well-defined oxidation peak and resistance-like  $i$  vs.  $E$  curve in the region where  $Li^+$  insertion occurs, with a change of electrode coloration from transparent to blue well visible by naked eye. The reader can easily see the effect of the length of the nanorolls on the shape of oxidation peak in Figure 4. When a higher Molecular weight PVA (85000-124000 M.W.) is employed in seed layer preparation the resulting nanorolls are longer than those obtained by using lower M. W. PVA (31000-50000 M.W.).

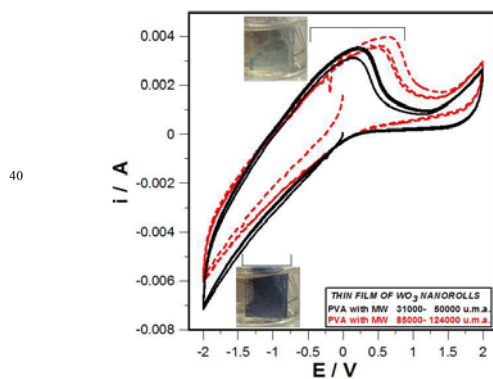


**Figure 4.** Cyclic Voltammogram of  $WO_3$  Nanorolls film on FTO with typical color appearance and effect of the length of the nanowires on the shape of oxidation peak. Electrolyte: LiTFSi 1 M in PC. Electrodes setup:  $WO_3$  NR on FTO as Working, Platinum plate as counter and Ag/AgCl electrode as reference. Scan rate : 0.1 V/s.

As confirmation the samples employed in CV were observed at FESEM showing a thickness of the  $WO_3$  nanorolls layer of 807 nm and 360 nm respectively (Figure S1). When the  $WO_3$  fibres are longer their oxidation peak in CV is broadened toward the

region of positive potentials; this could be due to the presence of a higher amount of  $WO_3$  redox centres that are more distant from the FTO layer with a different electrochemical neighbourhood.

To monitor the effect of the  $Li^+$  insertion and de-insertion on the UV-VIS light absorption, the typical spectrum of  $WO_3$  nanorolls on FTO glass has been registered in 1 M LiTFSi PC solution after biasing for 1 minute at different potential (Figure 5 left). The UV-VIS spectrum was recorded at potentials ranging from 0 V to -2.5V (vs. Ag/AgCl). In the negative potentials region, the electrode becomes progressively more intensely coloured ( $T\%$  decrease), as it is clearly evident from  $\Delta T\%$  in 350-1000 nm interval. The change in colour was already detectable by naked eye at -1V; with a bias of -2 V the colour change was almost complete. To estimate the switching times, steps of negative and positive potential have been sequentially applied for several cycles with the following program:  $E_1 = +0$  V,  $E_2 = -2$  V vs. Ag/AgCl ;  $t_1 = t_2 = 40$  s (Figure 5 Right). According to the definition given in S. I. we found for nanorolls/FTO electrodes  $ST_B = 8$  s and  $ST_C = 9$  s. The differences between  $ST_B$  and  $ST_C$  are in general due to surface charge effect on the rate of  $Li^+$  intercalation/extraction<sup>25</sup>. The results seems to indicate that the surface charge of  $WO_3$  nanorolls is positive and there is a slight repulsive electrostatic field that slow down  $Li^+$  insertion and facilitate  $Li^+$  extraction from  $WO_3$  thin layer.” To test the durability of electrochromic performances the effect of 2000 cycles on the switching time and contrast of the  $WO_3$  NR electrode has been studied in 1M LiTFSi PC solution by summarizing the basic opto-electrochemical features in Table S2. The experiments evidenced the stability of the switching times and an acceptable decrease of contrast (ca. 80 % of initial  $\Delta T\%$ (550 nm) and  $\Delta T\%$ (700 nm) after 2000 cycles) suggesting a certain structural stability of the thin layer during prolonged electrochemical switching in solution.

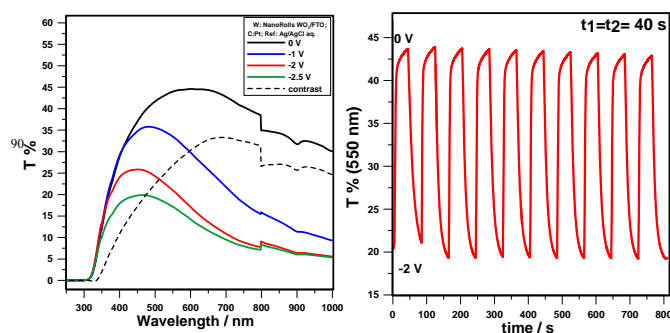


**Figure 5.** Spectroelectrochemical features of  $WO_3$  NR thin film. (Left) Typical Spectrum vs.  $E$ ; (Right)  $T\%$ (550) vs. time for ten cycles of bleaching and colouring. Electrolyte: LiTFSi 1 M in Propylene Carbonate. Electrodes setup: Nanorolls film on FTO as Working, Platinum plate as counter and Ag/AgCl electrode as reference. Finally the coloration efficiency was measured at 700 nm for the three types of  $WO_3$  NR (Low, middle and high M.W. PVA) and compared with  $WO_3$  nanoflakes prepared by us with the Su method<sup>17</sup>. The results are summarized in a Table S3. For  $WO_3$  NR  $\eta$  was found in the range of 39-67  $cm^2C^{-1}$  very similar to that of nanoflakes of 60  $cm^2C^{-1}$  showing the low energy consumption of the novel nanocrystalline thin layers.

## Conclusions

In summary novel nanocrystals i.e. WO<sub>3</sub> nanorolls were self-assembled on FTO/glass by a quick and HCl free hydrothermal synthesis. The WO<sub>3</sub> nanorolls, as evidenced by FESEM and HR-TEM analysis are fibrous nano-structures made of rolled nanoflakes with a telescope-like ending portion. Due to their nano-porosity, excellent electrochemical accessibility and to the envisaged presence of nanocavities between the rolled layers, the thin films of WO<sub>3</sub> nanorolls obtained here hold tremendous promise for nano-electronics, electrochromic devices, water photo-splitting cells, Li-ion batteries and nano-templated filters for UV radiation.

This research has been carried out in the context of the FP7 European Project “RESSEEPE”(Grant Agreement no: 609377). EU community is kindly acknowledged for the financial support.

<sup>a</sup> GAME Lab, Dept. Applied Science and Technology - DISAT, Politecnico di Torino, Italy. Fax: +39 011 0904699; Tel: +39 011 0904641; E-mail: simone.zanarini@polito.it, silvia.bodoardo@polito.it  
<sup>b</sup> Dipartimento di Scienze della Terra, Università di Torino, Torino, Italy  
<sup>c</sup> NIS Centre of Excellence, Università di Torino, Torino, Italy.

† Electronic Supplementary Information (ESI) available: Characterization Techniques; Additional FESEM micrographs; Typical XRD pattern of WO<sub>3</sub> nanorolls thin film; Typical Nyquist Plots at ambient temperature; Indicative diameter and length of WO<sub>3</sub> NR by varying PVA chain length; Effect of 2000 cycles of electrochemical switching on the ST<sub>B</sub>, ST<sub>C</sub> and ΔT%; Coloration Efficiency of the WO<sub>3</sub> NR.

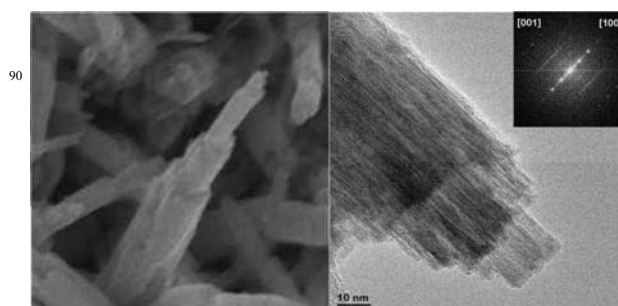
## Notes and references

- 1 C. G. Granqvist, *Handbook of Inorganic Electrochromic Materials*, 2002, Elsevier, Amsterdam.
- 2 C. G. Granqvist, *Thin Solid Films*, 2014, **564**, 1-38.
- 3 C. M. White, D. T. Gillaspie, E. Whitney, S-H. Leea, A. C. Dillon, *Thin Solid Films*, 2009, **517**, 3596-3599.
- 4 D. Xu, T. Jiang, D. Wang, L. Chen, L. Zhang, Z. Fu, L. Wang, T. Xie, *ACS Appl. Mater. Interfaces*, 2014, **6**, 9321-9327.
- 5 M. G. C. Zoontjes, M. J. Huijben, W. G. Baltrusaitis, *ACS Appl. Mater. Interfaces*, 2013, **5**, 13050-13054.
- 6 S. Yoon, C. Jo, S. Y. Noh, C. W. Lee, J. H. Song, *Phys. Chem. Chem. Phys.*, 2011, **13**, 11060-11066.
- 7 S. Zhuiykov, E. Kats, B. Carey, S. Balendhran, *Nanoscale*, 2014, **6**, 15029-15036.
- 8 S. K. Deb, *Sol. Energy Mater. Sol. Cells*, 2008, **92**, 245-258.
- 9 M. Deepa, M. Jikar, D. P. Singh, A. K. Sristava, A. Shahzada, *Sol. Energy Mater. Sol. Cells*, 2008, **92**, 170-178.
- 10 G. F. Cai, J. P. Tu, D. Zhou, X. L. Wang, C. D. Gu, *Solar Energy Mater. Solar Cells*, 2014, **124**, 103-110.
- 11 V. V. Kondalkar, S. S. M. Kharade, K. V. Khot, P. B. Patil, R. M. Mane, *Dalton Trans.*, 2015, **44**, 2788-2800.
- 12 J. Zhang, J. P. Tu, G. F. Cai, G. H. Du, X. L. Wang, P. C. Liu, *Electrochim. Acta*, 2013, **99**, 1-8.
- 13 D. Ma, G. Shi, H. Wang, Q. Zhang, Y. Li, *J. Mater. Chem. A*, 2013, **1**, 684-691.
- 14 K. Huang, Q. Pan, F. Yang, S. Ni, X. Wei, D. He, *J. Phys. D: Appl. Phys.*, 2008, **41**, 155417-155422.
- 15 N. Huo, S. Yang, Z. Wei, J. Li, *J. Mater. Chem. C*, 2013, **1**, 3999-4004.
- 16 J-W. Liu, J. Zheng, J-L. Wang, J. Xu, H-H. Li, S-H. Yu, *Nano Letters*, 2013, **13**, 3589-3593.

- 17 J. Su, X. Feng, J. D. Sloppy, L. Guo, C. A. Grimes, *Nano Letters*, 2011, **11**, 203-208.
- 18 H. Li, G. Shi, H. Wang, Q. Zhang, Y. Li, *J. Mater. Chem. A*, 2014, **2**, 11305-11310.
- 19 G. Xi, J. Ye, Q. Ma, N. Su, H. Bai, C. Wang, *J. Am. Chem. Soc.*, 2012, **134**, 6508-6511.
- 20 C. Yan, W. Kang, J. Wang, M. Cui, X. Wang, C. Y. Foo, K. J. Chee, P. S. Lee, *ACS Nano*, 2014, **1**, 316-322.
- 21 N. Kumagai, A. Yu, N. Kumagai, H. Yashiro, *Thermochimica Acta*, 1997, **299**, 19-25.
- 22 M. Hibino, W. Han, T. Kudo, *Solid State Ionics*, 2000, **135**, 61-69.
- 23 S. Balaji, Y. Djaoued, A.-S. Albert, R. Z. Ferguson, R. Brüning, *Chemistry of Materials*, 2009, **21**(7), 1381-1389.
- 24 L.B. Valdes, *Proc. I.R.E.*, 1954, **42**, 420-427.
- 25 P. M. S. Monk, R. J. Mortimer, D. R. Rosseinsky, *Electrochromism and Electrochromic Devices*, 2007, Cambridge University Press, Cambridge.

**Keywords:** Nano-sized Crystals, Nanorolls, Tungsten Oxide, In Situ Hydrothermal Synthesis, Electrochromism, Nano Cavities, multi-layer nanostructures.

## Graphical Abstract:



## SUPPORTING INFORMATION

### **WO<sub>3</sub> Nanorolls Self-Assembled as Thin Films by Hydrothermal Synthesis**

S. Vankova<sup>a</sup>, S. Zanarini<sup>a\*</sup>, J. Amici<sup>a</sup>, Fernando Cámara<sup>b,c</sup>, Rossella Arletti<sup>b,c</sup>,  
S. Bodoardo<sup>a</sup>, N. Penazzi<sup>a</sup>

<sup>a</sup> Department of Applied Science and Technology - DISAT, Politecnico di Torino, C.so Duca degli Abruzzi 24, 10129 Torino, Italy.

<sup>b</sup> Dipartimento di Scienze della Terra, Università di Torino, via Valperga Caluso 35, 10125, Torino, Italy.

<sup>c</sup> NIS Centre of Excellence, Università di Torino, Via Giuria 7, 10125 Torino, Italy.

#### **Characterization techniques**

CH Instrument 600D Station (galvanostat/potentiostat, CHI instruments, Austin, USA) was used for electrochemical and opto-electrochemical measurements, by registering current vs. potential and current vs. time curves. Cyclic voltammeteries of the cathodes were registered in 1 M Lithium bis-trifluoromethanesulfonimide (LiTFSI) in Propylene Carbonate (PC) with a standard three electrode cell with WO<sub>3</sub> nanorolls thin film on ITO glass as working electrode, a Platinum plate as counter electrode and an Ag/AgCl electrode as reference. Spectro-electrochemical measurements were carried out by placing the custom-made cell in the sample compartment of a Varian Cary 500 UV-VIS spectrophotometer. Two different types of measurement were performed by coupling the spectrophotometer with the CH 600D potentiostat. The first type of experiment was the registration of the complete UV-VIS absorption spectrum as function of applied potential; the second type of experiment consisted in the acquisition of the visible light absorption at a specific wavelength as function of time during potential modulation i. e. repeated bleaching and coloring cycles. The switching time for Bleaching ( $ST_B$ ) and the switching time for coloring ( $ST_C$ ) can be easily calculated from the T% vs. time curves by the time necessary after bias inversion to reach the 80% of the maximum (bleaching, oxidation) or minimum (coloring, reduction) T% starting from

previous potential step minimum or maximum T% respectively. The electrochemical impedance spectroscopy (EIS) response was analyzed in the frequency range 10 mHz - 1 MHz at the open circuit potential, using the previously described CH 600D potentiostat equipped with a proprietary fitting software.

The morphology of the products was observed by field emission scanning electron microscopy (FESEM, Hitachi S-4300SE). The crystallographic phases of the fabricated thin films were examined by X-ray diffraction (XRD, Philips X'pert MRD diffractometer) using Cu K $\alpha$  radiation. The size and crystal structure of the hydrothermally-grown WO<sub>3</sub> nanorolls were also confirmed by high resolution transmission electron microscopy (HR-TEM), selected area electron diffraction (SAED) using a JEOL Jem 3010 uhr, working at 300 kV, a LaB6 source and a Gatan CCD camera attached. Sample was dropped on a copper mounted holey carbon film.

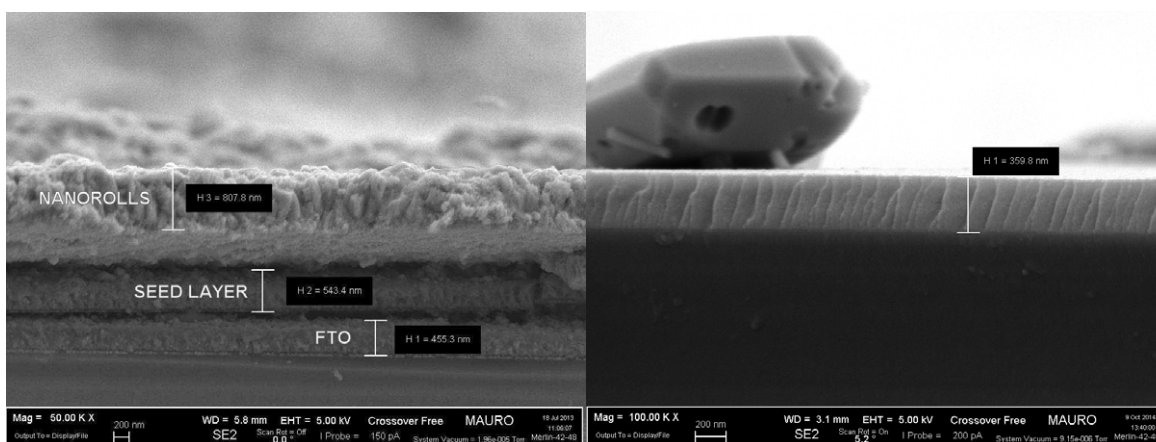


**Figure S1.** (left) FESEM micrograph showing the typical layer-by-layer aspect of the thin layer of WO<sub>3</sub> nanorolls obtained here. The seed layer was obtained with PVA of 85-124 000 u. m. a. ; (right) Cross section of a thin layer of WO<sub>3</sub> nanorolls with seed layer obtained with PVA of 31000-50000 u. m. a. .



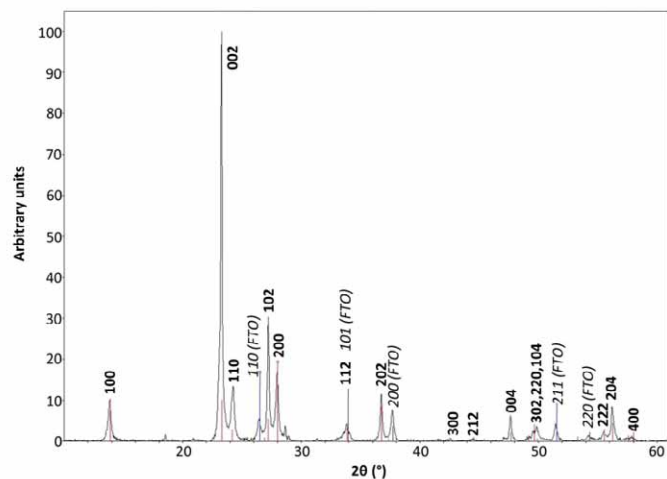


**Figure S2.** Typical XRD pattern of  $\text{WO}_3$  nanorolls thin film on FTO/glass substrate.

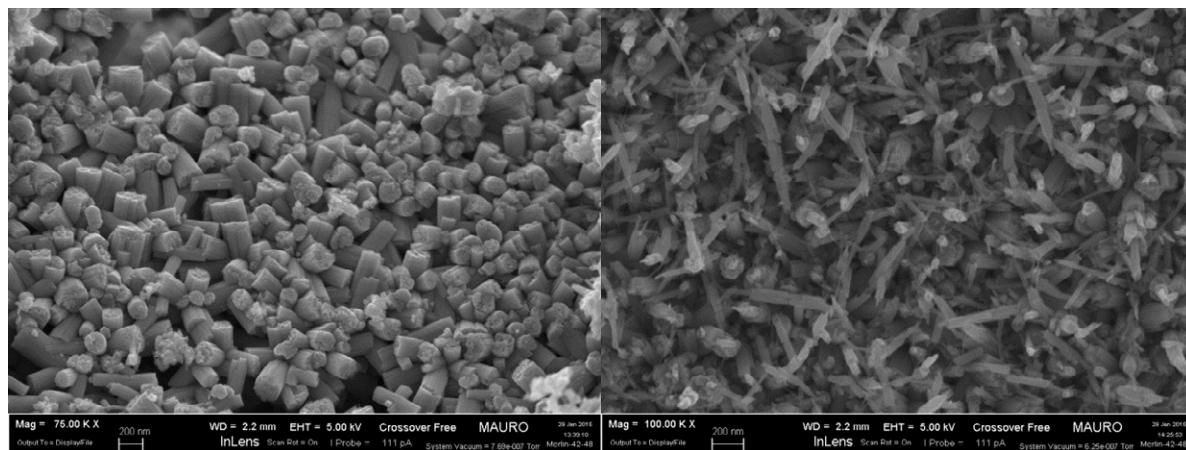


**Figure S3.** (Left) FESEM Picture showing the typical firewood-like fragmented  $\text{WO}_3$  nanorolls (shorter PVA Chain) obtained by scratching away the thin layer on Lacey Carbon/200 nm Cu mesh; (right) FESEM shot showing the typical elongated and thinner structure of  $\text{WO}_3$  NR on FTO glass (longer PVA chain).

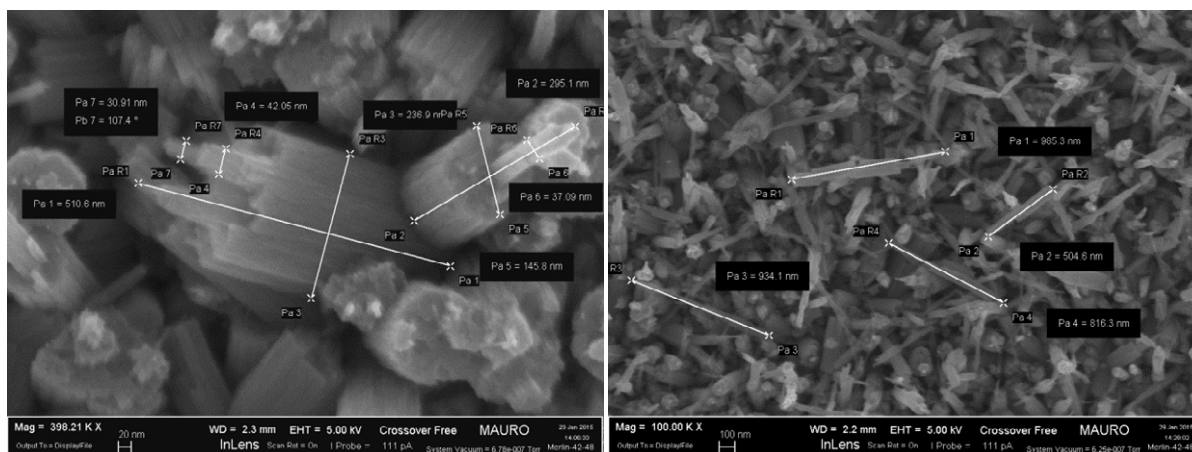


**Figure S4.** FESEM Pictures showing examples of measurement of diameter and length of the  $\text{WO}_3$  NR obtained in different preparative conditions.

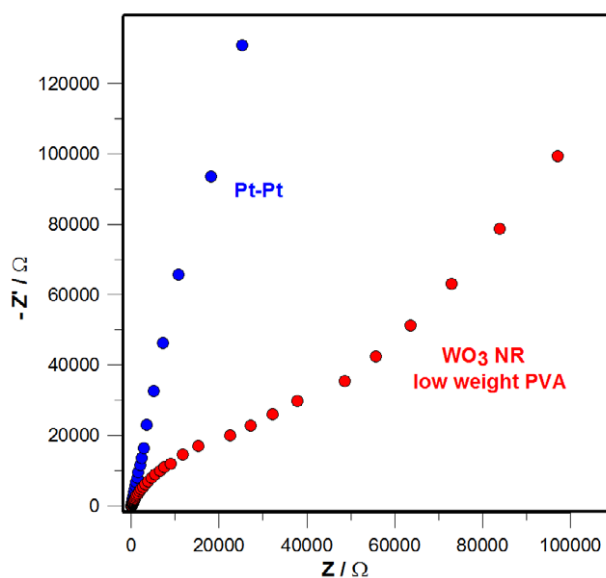


**Figure S5.** Typical Nyquist Plots at ambient temperature in PC 1M LiTFSi solution. Electrodes setup: (blue dots ) Pt plate | Pt plate | Ag/AgCl reference and (red dots)  $\text{WO}_3$  nanorolls/FTO | Pt plate | Ag/AgCl reference. Frequency range: 10 mHz - 1 MHz at the open circuit potential.

PVA Chain weight / UMA	Overall $\text{WO}_3$ NR length / nm	Log portion length / nm	Log portion diameter / nm	Tip portion diameter / nm
31000-50000	300-650	200-600	200-300	20-50
85000-124000	500-900	200-500	75-150	20-50
146000-186000	750-1300	650-1200	75-150	20-50

**Table S1.** Indicative diameter and length of  $\text{WO}_3$  NR by varying PVA chain length in seed layer preparation. These range values are based on 20 single NR measurements taken by FESEM pictures.

<b>WO<sub>3</sub> NR/ glass FTO</b>	<b>Cycle nr. 5</b>	<b>Cycle nr. 2000</b>
<b>ST<sub>B</sub><sup>I</sup></b>	8 s	8 s
<b>ST<sub>C</sub><sup>II</sup></b>	9 s	9 s
<b>ΔT%(550 nm)</b>	26 %	21 %
<b>ΔT%(700 nm)</b>	33 %	27 %

<sup>I</sup> Switching Time of bleaching for 80% ΔT%max at 550 nm by applying a potential of -2 to 0V vs. Ag/AgCl.

<sup>II</sup> Switching Time of coloring for 80% ΔT%max at 550 nm by applying a potential of 0 to -2V vs. Ag/AgCl.

**Table S2.** Effect of 2000 cycles of electrochemical switching on the **ST<sub>B</sub>**, **ST<sub>C</sub>** and **ΔT%** of WO<sub>3</sub> nanorolls . Electrolyte: LiTFSI 1 M in Propylene Carbonate. Electrodes setup: Nanorolls film on glass FTO (low M.W. PVA) as Working, Platinum plate as counter and Ag/AgCl electrode as reference. Potential program: E<sub>1</sub>= +0 V, E<sub>2</sub>= -2 V; t<sub>1</sub>=t<sub>2</sub>=40 s.

<b>Nanocrystal type</b>	<b>Coloration Efficiency η (cm<sup>2</sup>C<sup>-1</sup>)<sup>*</sup></b>
<b>WO<sub>3</sub> nanoflakes</b>	60±8
<b>WO<sub>3</sub> nanorolls (M.W. PVA= 31000-50000)</b>	67±6
<b>WO<sub>3</sub> nanorolls (M.W. PVA= 85000-124000)</b>	53±5
<b>WO<sub>3</sub> nanorolls (M.W. PVA= 146000-186000)</b>	39±7

\* based on 5 different samples of each type

**Table S3.** Coloration Efficiency of the WO<sub>3</sub> NR produced by HT synthesis in different conditions and comparison with WO<sub>3</sub> nanoflakes produced by the Su method.